CI

e-med
www.e-med.org.uk

REVIEW

Potential of compressed sensing in quantitative MR imaging of cancer

David S. Smith[a,b], Xia Li[a,b], Richard G. Abramson[a,b], C. Chad Quarles[a,b], Thomas E. Yankeelov[a–e], E. Brian Welch[a–c]

[a]*Institute of Imaging Science, Departments of* [b]*Radiology and Radiological Sciences,* [c]*Biomedical Engineering,* [d]*Physics and Astronomy, and* [e]*Cancer Biology, Vanderbilt University, Nashville, TN, USA*

Corresponding address: E. Brian Welch, Vanderbilt University Institute of Imaging Science, 1161 21st Avenue South, AA 1105 Medical Center North, Nashville, TN 37232–2310, USA.
Email: brian.welch@vanderbilt.edu

Abstract

Classic signal processing theory dictates that, in order to faithfully reconstruct a band-limited signal (e.g., an image), the sampling rate must be at least twice the maximum frequency contained within the signal, i.e., the Nyquist frequency. Recent developments in applied mathematics, however, have shown that it is often possible to reconstruct signals sampled below the Nyquist rate. This new method of compressed sensing (CS) requires that the signal have a concise and extremely dense representation in some mathematical basis. Magnetic resonance imaging (MRI) is particularly well suited for CS approaches, owing to the flexibility of data collection in the spatial frequency (Fourier) domain available in most MRI protocols. With custom CS acquisition and reconstruction strategies, one can quickly obtain a small subset of the full data and then iteratively reconstruct images that are consistent with the acquired data and sparse by some measure. Successful use of CS results in a substantial decrease in the time required to collect an individual image. This extra time can then be harnessed to increase spatial resolution, temporal resolution, signal-to-noise, or any combination of the three. In this article, we first review the salient features of CS theory and then discuss the specific barriers confronting CS before it can be readily incorporated into clinical quantitative MRI studies of cancer. We finally illustrate applications of the technique by describing examples of CS in dynamic contrast-enhanced MRI and dynamic susceptibility contrast MRI.

Keywords: *Compressed sensing; compressive sampling; compressive sensing; quantitative MRI; cancer; clinical trials; dynamic contrast-enhanced; dynamic susceptibility contrast.*

Introduction

There is a wide array of noninvasive quantitative imaging biomarkers currently under development for incorporation into clinical trials. The hope of these emerging techniques is that they will provide more sensitive and specific information on the response of a range of cancers to therapy. Many of these promising methods currently require acquisition parameters that can be quite demanding; more specifically, the spatial resolution, temporal resolution, and signal-to-noise requirements can be challenging to satisfy in the clinical setting. Thus, it is imperative that the field develops and validates broadly applicable image acquisition methods that can maximize these 3 key imaging parameters. Unfortunately, optimizing any 1 of these 3 parameters almost always requires suboptimal settings for the other two. New methods are needed to alleviate this fundamental issue in the acquisition of magnetic resonance (MR) images. One very promising technique to address this challenge is compressed sensing (CS).

MR imaging (MRI) has stood out in the field of CS as one of the early successes. Since MR scanner measurements are performed in the Fourier (spatial frequency) domain, MR acquisitions are already fundamentally compatible with the random sampling in an incoherent basis required by CS sensing theory. CS can reduce the data collection burden of MRI sequences by a factor dependent on the ability of the data to be compressed in some domain. Any improvement in data collection efficiency

can be translated into improvements in image quality and the usefulness of derived quantitative parameters.

In the next section, we review the theory and early applications of CS in several non-quantitative MRI techniques. the third, we discuss special CS considerations that need to be addressed before the approach can be readily incorporated into cancer clinical trials and implemented in advanced imaging centers. Finally, we discuss 2 immediate applications of CS to quantitative MRI (qMRI), specifically dynamic contrast-enhanced (DCE) MRI and dynamic susceptibility contrast (DSC) MRI.

CS in MRI

Theory of CS

CS describes the use of information about a signal's structure to allow complete signal reconstruction despite incomplete sampling[1–3]. The prototypical example is a structured time series signal that is subsampled with respect to the Shannon–Nyquist sampling theorem, which dictates a sampling rate of at least twice the largest frequency component in the band-limited signal. The signal structure that most often permits undersampling is a sparse signal. A sparse signal is defined as a signal that can be represented in some (possibly unknown) mathematical basis with far fewer vector components than in its natural basis (e.g., space, time, frequency). We extend the scope of this terminology here to define a compressible signal as one that has a sparse representation in which the signal may be approximated to high, but not perfect, accuracy. A common example of signal compression is the JPEG2000 encoding of photographic images.

The reconstruction of these structured signals is usually performed with an iterative least-squares optimization in which a sparsity-promoting norm serves as an additional constraint, or regularizer. This formulation prefers solutions that exhibit structure, and has been recently proved to correctly reconstruct sparse signals under certain circumstances[1–3]. The most common sparsity-promoting norm is the l_1-norm, defined as

$$\|\mathbf{x}\|_1 \equiv \sum_i |\mathbf{x}_i|$$

which is the sum of magnitudes of the components of a vector. This yields the common CS optimization problem

$$\hat{\mathbf{x}} = \arg\min_{\mathbf{x}} \|\mathbf{x}\|_1 + \frac{\lambda}{2} \|A\mathbf{x} - \mathbf{b}\|_2^2$$

where $\mathbf{x}$ is a sparse representation of the data and A is a measurement operator that transforms the sparse representation to the data domain. This mathematical notation is shorthand for the optimization problem to find the $\mathbf{x}$ that minimizes the expression on the right-hand side. The solution will strike a balance between the sparsity promoted by the l_1-norm and fidelity to the measured data $\mathbf{b}$.

The l_1-norm is compatible with a wide array of convex optimization algorithms that can provide very rapidly converging solutions, contributing to the popularity of this formulation. This is important to MRI because the dimensionality of the problem is of the order of the number of voxels acquired, typically 10^6 or more, and possibly much higher for dynamic or multiparametric data sets. Hence almost all CS MRI problems require large-scale optimization algorithms.

In MRI, the measurements are acquired in the spatial frequency domain (Fourier transform domain), so the CS problem can be reformulated as

$$\hat{\mathbf{x}} = \arg\min_{\mathbf{x}} \|\mathbf{x}\|_1 + \frac{\lambda}{2} \|F_u S^{-1} \mathbf{x} - \mathbf{b}\|_2^2$$

where the measurement operator F_u is an undersampled discrete Fourier transform, S^{-1} is the inverse of the sparsifying transform (takes the sparse representation into the image domain), and the sparse representation $\mathbf{x}$ is typically a wavelet or gradient decomposition. Note that MR images are not sparse in any currently known domain, so it is more accurate to refer to them as compressible. Specifically, an anatomic MRI image can often be represented with fewer wavelet or gradient coefficients than the number of pixels in the image itself with only minimal compression error. One of the primary determinants of the compression error is the level of noise in the image, measured in MRI by the signal-to-noise ratio (SNR). Noise in MRI is approximately Gaussian, with uniform power (white noise) in the Fourier domain and Rician in the spatial domain magnitude image, so it lacks large-scale structure and is thus difficult to represent by any sparsifying basis.

CS usually requires a random measurement to be performed. In MRI, the object is sampled in the Fourier domain as a number of spatial frequency encoded readouts. These readouts may be linear, if the gradient is constant, or curved, if the gradient is time varying. However, the fundamental building block of all MRI measurements is the readout "line," which is understood to refer to all arbitrary sampling trajectories of any curvilinear shape. Within this constraint, we are free to choose the number of readouts and their associated trajectory shapes. For a Cartesian acquisition scheme, the readouts will be parallel lines spaced along 1 or 2 phase encode directions. Fig. 1 shows an example of a simulated CS-undersampled 2-dimensional (2D) Cartesian measurement on a Shepp–Logan phantom. Random undersampling according to CS then requires that a subset of these lines be selected for sampling, with their spacing dictating the field of view of the image and the maximum spatial frequency encoded dictating the spatial resolution. The missing phase-encoded lines lead to "ghosting" of image power across the field of view. This incorrectly localized power is then replaced by the CS reconstruction. For radial and spiral readout trajectories, one may angularly undersample by regularly discarding readout trajectory
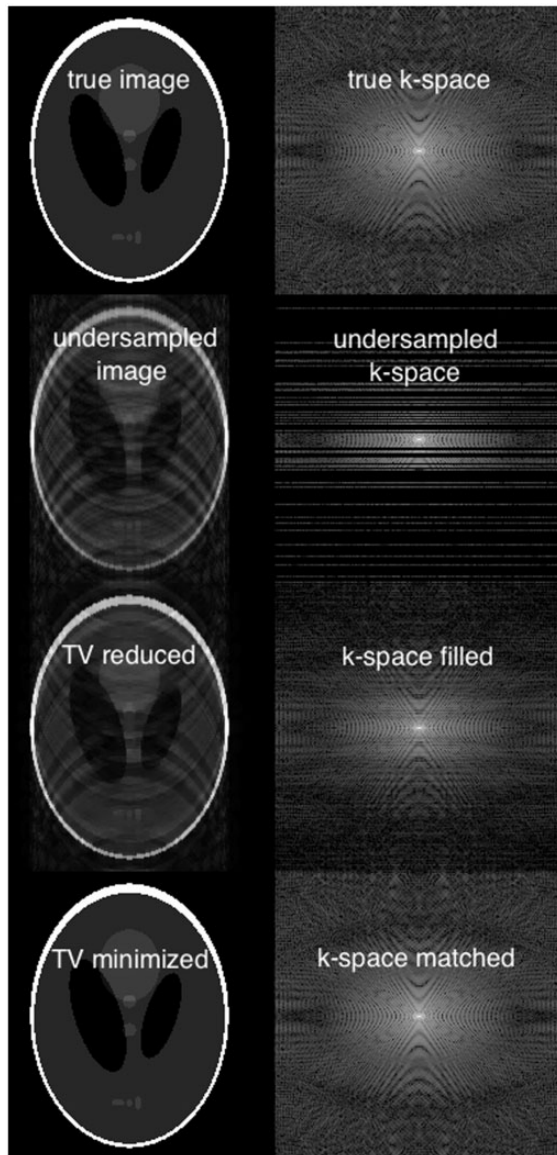
Figure 1 **The essential feature of compressed sensing is that part of the measurement in k-space is not performed. Here we show the simulated two-dimensional (2D) Cartesian undersampling of a Shepp–Logan phantom. Since 2D MRI scans are restricted to either acquiring or omitting entire readout lines, random rows of the data have been discarded to create the undersampled k-space. Then, after data acquisition, the missing data are replaced by the results of an optimization that minimizes aliasing artifacts in the reconstructed image. The fully sampled image is shown in the top row, while the second through bottom rows show the initial undersampling followed by successive steps in the reconstruction. Here the constraint on the image sparsity is the TV, or total variation, which is the sum of pixel magnitudes in the gradient image.**

acquisition angles. Undersampling of a non-Cartesian acquisition normally leads to complicated aliasing and blurring artifacts in the image. However, such artifacts can be removed by CS reconstruction. All of these acquisition patterns have been successfully employed in MR to achieve significant reductions in the data acquisition burden (e.g., Ref.[4]).

Initial applications of CS to MRI

Soon after the formalization of CS theory in 2006[1,2], CS was applied to medical imaging. In fact, an example of image reconstruction with a limited number of spatial domain projections, theoretically similar to data obtainable in several tomographic medical imaging modalities such as X-ray computed tomography (CT), single-photon emission CT, positron emission tomography, and radial MRI, was prominently presented by Candès et al.[11]. Among all medical imaging modalities, MRI is the most compatible with CS methodology because of the flexibility in which MRI encodes and collects data directly in the spatial frequency domain.

To date, the vast majority of CS-related biomedical imaging research uses MRI. The first publication from the MR community using CS theory appeared in 2007,[5] and included CS-accelerated reconstructions of anatomic brain images and contrast-enhanced MR angiography (CE-MRA). Among MR applications, CE-MRA is particularly well suited for CS acceleration because of the inherent image domain sparsity associated with bright vessels with sharp edges superimposed on dark background tissue. The next MR application to harness CS was dynamic cardiac MRI[6,7], which has traditionally been a demanding application and a long-standing subject of MR research. Many techniques for fast scanning, coherent undersampling, and various data-sharing methods had already been applied to dynamic cardiac MRI, but CS opened a new avenue for data acquisition acceleration. Furthermore, the dynamic nature of cardiac MRI yielded an additional dimension along which CS sparsity constraints could be applied.

The immense potential of CS in MRI was quickly recognized, and in 2008 it began to be applied to MR spectroscopic imaging (MRSI) of hyperpolarized ^{13}C[8,9]. By 2010 many more applications were reported. Ajraoui et al.[10] applied CS to lung MRI using hyperpolarized helium. Doneva et al.[11] developed CS-accelerated versions of traditionally time-consuming parametric mapping of tissue parameters such as T_1 and T_2 in the brain as well as accelerated abdominal fat-water imaging[12]. Other cardiac applications such as cardiac perfusion[13] were explored. Jung and Ye[14] published a CS-based method for motion estimation and compensation of brain and cardiac MRI. Brain applications also continued to harness CS, including diffusion MRI[15]. Several investigators pursued new contrast-enhanced MRI applications to combine with CS, such as 3-dimensional (3D) DCE-MRI[16] and DCE-MRI of the breast[17,18].

The rapid pace of CS development for MRI accelerated further in 2011 from groups tackling challenges such as joint reconstruction of multiple brain image

contrasts[19], motion compensated free-breathing coronary MRI[20], whole-brain susceptibility mapping[21], brain diffusion spectrum imaging[22], 4-dimensional contrast-enhanced MRA of brain and lower extremities[23], low-contrast detectability in spine imaging[24], coronary MRI[25], and brain functional connectivity[26]. Improved anatomic imaging was targeted for brain and musculoskeletal[27], cardiac[28], breast[29], and spine[30]. Despite the widespread and growing exploration of CS in a broad range of MR research applications, published reports continue to be dominated by phantom and brain imaging, which present fewer implementation and deployment challenges, as well as by retrospective studies in which fully sampled raw data sets are down-sampled after data collection. More studies are needed to demonstrate robust and high image quality in prospectively under-sampled CS-accelerated scans of the challenging anatomy characteristic of many clinical trial protocols, such as body imaging, low-contrast anatomy, and targets likely to be confounded by artifacts such as motion.

Considerations for incorporating CS MRI into cancer clinical trials

Expectations for quantitative MRI in clinical trials

Before we address the utilization of CS in clinical trial imaging, we first outline the motivations for using qMRI in clinical cancer trials. Clinical cancer trials are now at an important crossroads, with focus shifting from establishing the basic rules and paradigms for response assessment to critically examining current response assessment tools for deficiencies and possible improvements. Starting with the first clinical trials of chemotherapy for solid tumors in the 1960s, an international consensus slowly emerged around a basic response assessment paradigm using discrete response categories (complete response, partial response, stable disease, progressive disease) defined by objective measurement rather than subjective perception. Standards for solid tumor evaluation were codified first in the World Health Organization criteria[31] and subsequently in the Response Criteria for Solid Tumors (RECIST)[32] with later modification as RECIST 1.1[33]. Standards for hematologic malignancies were also established and refined[34,35]. These criteria, which focus on changes in lesion size measurement over time, have become the standards for virtually all clinical trials in which imaging-based response evaluation is sought.

Recently, however, these size-based techniques have come under increasing scrutiny, and several important deficiencies have been brought to light. RECIST sets out rigorous rules for defining which lesions can be measured and followed over time, explicitly excluding infiltrative lesions or discrete lesions that are too small to qualify for measurement. For lesions that do qualify as target lesions for measurement and follow-up, it can be difficult for the observer to choose a representative tumor burden, and it can be challenging to measure lesions along curved surfaces or abutting other organs or pathology. Linear measurements alone may not adequately capture size changes in nonspherical or asymmetric lesions, and both intraobserver and interobserver measurement variability can be high, especially for heterogeneous lesions or lesions with irregular borders[36].

However, perhaps the most important challenge to traditional size-based response assessment is the notion that size measurement criteria may underestimate or fail to capture the antitumor efficacy of some agents, especially newer targeted therapies that produce a cytostatic rather than a cytotoxic effect[37,38]. For some newer anticancer agents, change in tumor size may lag weeks to months behind tumor behavioral response or may never occur at all. An exclusive focus on tumor size may also exclude other potentially meaningful tumor characteristics, including morphologic (density, necrosis, calcification, heterogeneity), compositional (biochemical, molecular), and functional (vascular perfusion, energy metabolism, DNA synthesis) parameters.

Given these observations, there has been a recent surge in experimental testing of quantitative imaging biomarkers for response assessment. Many of these newer biomarkers are MRI-based, and use advanced imaging techniques to interrogate tumors on a molecular and functional level. Examples of MRI-based advanced response biomarkers include DCE-MRI and DSC-MRI for evaluation of tumor angiogenesis[39], diffusion-weighted (DW)-MRI for evaluation of tumor cellularity[40], MR spectroscopy for interrogation of phospholipid metabolism associated with cell membrane turnover[41], and blood-oxygen-level dependent (BOLD)-MRI for evaluation of tumor hypoxia[42]. All of these techniques offer quantitative information on tumor response that could potentially be incorporated into cancer clinical trials.

For these techniques to gain wide acceptance, certain criteria must be fulfilled. First, newer biomarkers must be validated in large clinical trials and must be shown to be comparable or superior to currently accepted methods. Newer biomarkers will be evaluated and compared with current methods along 3 major effectiveness metrics: ability to predict the natural course of disease (prognostic biomarkers), ability to predict sensitivity or resistance of disease to particular treatments (predictive biomarkers), and ability to identify treatment response or failure earlier and/or more accurately than current methods (early response biomarkers)[43]. CS techniques will likely play an important role in facilitating biomarker development by pushing the boundaries of spatial resolution, temporal resolution, and SNR. Assessment of evolving quantitative techniques will require validation of numerical thresholds, demonstration of acceptable sensitivity and specificity levels, and assessment of measurement error[44].

Second, qMRI biomarkers must be standardized to facilitate comparison of response data within a clinical trial, between different sites in a multicenter trial, and between different trials. This will require that MRI techniques be robust and reproducible across different platforms and equipment, and will require standardization of data acquisition and analysis methods. It will be incumbent upon researchers to specify their methods and imaging parameters with sufficient detail, and manufacturers will be called upon to reveal and disseminate technical details that previously may have been proprietary or confidential. CS methods will undoubtedly increase the complexity of the standardization process by introducing additional variables that must be held constant over the course of a trial and between trials. A number of organizations (including the Quantitative Imaging Biomarkers Alliance (QIBA) and the National Cancer Institute's Quantitative Imaging Network (QIN)) have been formed in an effort to facilitate dialogue between scan developers, clinicians, and manufacturers on standardization efforts.

Third, qMRI biomarkers must be reasonable to implement from a cost and availability perspective. At present, most imaging for cancer clinical trials is performed with CT (with the notable exception of neuro-oncology). This is most likely due to CT being cheaper and more widely available, along with the perception that CT offers easier image acquisition and fewer "moving parts" in terms of imaging parameters to be specified in trial protocols. In the near-term future, qMRI biomarkers will probably evolve within specialized advanced imaging centers linked to oncology cooperative groups and pharmaceutical industry partners; it will take much longer for these techniques to become ready for mass consumption in nonspecialized centers. Imaging researchers will therefore have to consider the most fruitful applications for biomarker development, with an emphasis on techniques for early-phase clinical trials that will facilitate earlier and more efficient selection of candidate drug agents for promotion to later-stage testing, as well as better identification of patients who will benefit from a particular drug.

Predictability and accuracy of CS MRI

The addition of CS to a clinical imaging protocol can also add unpredictability to the quality of the final image and the exact error in the associated calculated quantitative parameter maps[45]. The random nature of CS sampling schemes leads to less predictable performance for a given anatomic target. This is due directly to the magnitude of k-space coefficients varying from target to target. If an omitted coefficient would have had large amplitude for one target but not another, the final quality of the reconstructed image can vary greatly. For this reason, good CS acquisition methods should be optimized for a range of targets to be robust to these effects.

The SNR of a CS-based acquisition is a difficult question to address. Depending on the clinical application, a CS-enabled protocol may or may not improve the information content available to clinicians. Using CS can lead to both the loss of true signal (e.g., fine detail, producing compression artifacts) and the addition of false signal (aliased power from missing Fourier coefficients that does not get completely eliminated during reconstruction.) On the other hand, CS can also eliminate true noise by reducing low-magnitude coefficients in the sparse domain during reconstruction, and it can add true signal if the saving in acquisition time is used to acquire additional data, such as by averaging repeated data acquisitions or by acquiring new data at higher spatial frequencies than in the original non-CS protocol.

For example, in MRA CS has been revolutionary, with the ability to provide acceleration factors up to approximately 100-fold[46]. In MRA the goal is to create high-contrast images that are extremely sparse under a gradient transformation. This technique can tolerate a loss of fine features, because it requires only an essentially binary map of vessels, and it benefits from the reduction of system noise. Detection of cancer lesions, however, may prove difficult with CS because of the potential for loss of fine detail and contrast and the less predictable nature of undersampling artifacts. While the image artifacts due to flow, motion, and off-resonance are relatively easy to understand and disregard in the clinic, aliased power attributable to a suboptimal iterative reconstruction or excessive CS acceleration may be less predictable and harder to identify with any certainty. This could place practical limits on the ability of CS to improve some clinical protocols, and potentially reduce the sensitivity and specificity of non-quantitative imaging.

In quantitative MRI, the effects of CS manifest in the measurement error of quantitative parameters. This could also affect the statistical significance of measured parameters, possibly leading to altered power and sample-size requirements. Both clinical and research protocols must address this important statistical effect. Voxel-level data may have additional uncertainty added akin to the loss of fine details, or it may have less uncertainty if the data are accurately denoised. Quantitative parameters that have been averaged over a region or a group of voxels, such as tumor mean parameters, should have less error introduced by CS and should benefit from the denoising effect, since fine features will be averaged.

The loss of contrast caused by missing data in k-space and sparsifying constraints[47] could produce systematic error in quantitative parameter estimation, in at least DCE[45] and possibly other qMRI methods. Care must be taken to ensure that CS acquisition schemes minimize contrast loss. One common strategy is to bias the sampling densities in k-space toward low frequencies to mimic the distribution of power in k-space, which for anatomic images typically peaks at low spatial frequencies and diminishes to a roughly constant level at high frequencies. This sampling scheme ensures that the majority of signal in the largest k-space coefficients is

captured, thus maximizing the contrast of the reconstructed image.

The design of CS MRI protocols must find the proper balance of all of these concerns if they are to improve on existing non-CS-enabled sequences. Many of these issues should be easy to surmount with planning and optimization, but only prospectively implemented applications will be able to determine whether CS can provide a benefit. Much work remains to be done to characterize the competing effects on the accuracy and reliability of CS-based qMRI.

Practical deployment of CS in the clinical and research setting

The successful deployment of CS-accelerated MRI scans requires solutions to 6 primary workflow components: (1) CS sampling pattern design, (2) transmission and storage of the CS sampling pattern onto the MR scanner pulse sequence computer, (3) execution of the CS sampling pattern by the MR scanner pulse sequence computer, (4) transmission and storage of raw CS-accelerated data (along with information about the CS sampling pattern itself), (5) reconstruction of MR images from raw data, and (6) transmission and storage of reconstructed MR images into a desired image archive or database. Fig. 2 illustrates this workflow along with data transfer and storage requirements.

The first step in a CS-accelerated MRI workflow is the selection of the CS sampling pattern. In some cases, it may be possible to create a library of patterns in advance that are compatible with a range of MRI scan types and matrix sizes. However, the inherent flexibility of MRI for the customization of the field of view and spatial resolution, typically considered to be an advantage of the modality, makes it impractical to design CS sampling patterns in advance for all possible scans. Ultimately, the most desirable solution is a hybrid approach in which a large library of patterns is available along with the capability for on-demand generation of customized patterns. On-demand generation of CS sampling patterns also allows for customization of design algorithm parameters, which a user may want to refine to achieve a different balance of image quality characteristics.

Once a CS sampling pattern is selected, the details of that pattern must be conveyed to the MR scanner's pulse sequence computer. In the case of conventional CS-accelerated Cartesian MRI, the information about the locations of the Fourier domain phase-encoded readout lines is needed. A list of k_y values for 2D scans or (k_y, k_z) coordinates for 3D scans can be stored respectively as simple arrays of integers, a binary array, or even bit-masked unsigned integers if storage on the scanner hardware is limited. A tradeoff between ease of readability for users and compactness of storage must be made. Efficiency of the CS sampling pattern representation is more important as the number of patterns required for a scan increase, such as if different patterns are used for different 2D slices or 3D slabs, successive signal averages, dynamic repetitions, diffusion b-values, cardiac phase delays, MR echo times, or any other of many possible parameters that may be arrayed in a single MR imaging series. CS sampling patterns are unlike other simpler conventional sampling trajectories and patterns that can be described deterministically without the need for storing the entire pattern. In principle, knowing the algorithm and the random seed used to generate a pattern could allow reproduction of the pattern used, but this

Workflow Components for CS-Accelerated MRI

CS sampling pattern design	pattern storage & transmission	pattern execution on MR scanner	compressed raw data storage	iterative image reconstruction	transmission & storage of CS images
offline or MR console	MR console spectrometer	spectrometer	spectrometer & recon computer	recon computer or offline	MR console or DICOM PACS
10-100 MB	10-100 MB	10-100 MB	1-10 GB	1-10 GB	10-100 MB
human realtime: 0.1 sec	human realtime: 0.1 sec	spectrometer realtime: 10 μsec	fast: 0.1-1 GB/sec	medium: 1-10 sec	fast: 0.1-1 GB/sec

| LOCATION | REQUIRED MEMORY | MAXIMUM TIME LATENCY |

Figure 2 **Workflow components required to implement compressed sensing (CS) acquisitions into an MRI environment. Times and speed are approximate to illustrate the order-of-magnitude requirements. Many components must integrate into a balanced scheme in which no one component causes either a bandwidth or speed bottleneck, and sufficient software must be in place to seamlessly perform complex iterative CS reconstructions on the images midstream and to deposit the results into a clinical or research Picture Archiving and Communication System (PACS). DICOM, Digital Imaging and Communications in Medicine.**

may prove to be too unreliable for clinical needs, and storage of the raw pattern as part of the imaging data induces little overheard.

After the CS sampling pattern is made available to the MR pulse sequence computer, it must be incorporated into the execution of MRI pulse sequence. Conventional MRI protocols that sample Fourier domain data on a Cartesian grid typically acquire data as separate phase-encoded 1-dimensional (1D) lines. The location of the 1D frequency encoded readout in 2D or 3D k-space is changed with every repetition time (TR) of the pulse sequence. The order in which phase-encoded lines are acquired can easily be altered by the adjustment of the phase-encoding gradient waveform areas in each TR. Such flexibility is ideal for the acquisition of unconventional CS sampling patterns. Thus, standard spin-echo and gradient-echo MRI protocols that acquire 1 phase encode line per TR are relatively straightforward to modify to support CS. Challenges arise for other common MRI pulse sequence types that acquire multiple phase encodes in each TR such as turbo spin-echo, turbo field echo, gradient and spin-echo, and echo planar imaging. These so-called fast imaging techniques are carefully designed to satisfy gradient performance, pulse sequence timing, and human subject safety constraints. Constraints related to human subject safety are primarily limits on radiofrequency (RF) power, specific absorption rate, and peripheral nerve stimulation (PNS) caused by the rapid switching of magnetic field gradients. PNS limits commonly restrict the maximum slew rate duty cycle performed in fast MR imaging pulse sequences. It is imperative to obey such hardware and safety constraints to achieve the successful integration of CS sampling patterns with fast imaging pulse sequences.

The next task is to offload the acquired data to a workstation capable of performing a CS reconstruction. In modern MRI scanners, raw data can require several gigabytes of storage for a single scan, and this is likely to continue to increase. Multichannel-receive RF coils with up to 32 channels are increasingly prevalent, although with coil compression[48] the data can often be compressed into 6–8 "virtual coils." Given these sizes, direct raw data transmission links will likely require that the reconstruction workstation be placed in close proximity to the MR scanner with a dedicated high-speed connection to minimize data transfer delays. In addition to high bandwidth, the reconstruction workstation would ideally provide a large amount of random access memory (RAM) and a multicore central processing unit (CPU) or one or more graphics processing unit (GPU) boards. Large amounts of RAM are required for some CS reconstructions, especially those involving large, multicoil, dynamic data sets and/or those using low-rank constraints that require performing singular value decompositions. Smaller reconstructions can benefit from offloading onto GPU hardware for massively parallel execution of the matrix operations required.

For matrix sizes common in MRI, GPU-based CS reconstruction can yield acceleration of processing time by 25–30 times over CPU-based execution[49,50]. With the appropriate hardware and reconstruction algorithm choices, perhaps tailored to individual scans, reconstruction should not be a bottleneck to the clinical workflow.

Finally, the reconstructed MR images must be transmitted and stored in a database such as a Picture Archiving and Communication System (PACS) supporting the Digital Imaging and Communications in Medicine (DICOM) standard. The MR scanner console is typically the hub for image-data archival and is often connected to a remote DICOM PACS. All MR scanner consoles should be able to receive DICOM files; however, it may be impractical for the custom CS-accelerated MRI reconstruction workstation to form complete DICOM image files with all DICOM header metadata defined. Instead, many MR scanner vendors provide alternative routes for the reception of images into the console's database without the need for the DICOM format. Often such secondary image-reception paths use proprietary file formats unique to a scanner vendor. Although knowledge of the file format is needed, the proprietary formats typically require much fewer metadata compared with DICOM to associate the images with the correct patient, study, and examination. Second, the MR scanner console is already a multitasking machine used by the scanner operator to define, plan, and execute scanning protocols; view and process images; and archive data. Any additional network connectivity demand on the MR scanner console to receive images coming from an additional reconstruction workstation must be handled carefully so as not to cripple the other functions of the console.

The described challenges for deployment of CS in the clinical and research settings can be divided into obstacles that primarily require an engineering solution and problems that will likely remain areas for experimentation and optimization for years to come. Research prototypes and commercial products from scanner manufacturers to enable CS-accelerated MRI will almost certainly have different software and hardware solutions to overcome the somewhat mundane operations of transmission/storage of the CS sampling pattern, execution of the sampling pattern in the pulse sequence, and transmission/storage of specially reconstructed CS-accelerated MR images. Eventually the solutions to these straightforward challenges will be essentially hardcoded and built directly into the MR scanner. However, the remaining hurdles of CS sampling pattern design and reconstruction of images from raw CS-accelerated data will likely evolve iteratively over time, based on real-world feedback from radiologists and medical imaging physicists. Initial embodiments for CS-accelerated MRI will likely have many parameters to modify the sampling pattern and to control the reconstruction algorithm. However, flexibility and complexity should not

overshadow the need for a simple and robust implementation accessible to a broad user base. The more familiar clinicians and researchers are with the nature of CS-accelerated MRI, including the method's promise, limitations, and tradeoffs, the faster the field can converge on pragmatic strategies to overcome the obstacles to the widespread combination of CS with MRI.

Immediate quantitative applications for CS

Dynamic contrast-enhanced MRI

DCE-MRI is an umbrella term used to describe a variety of dynamic MRI techniques and analytical approaches, including both qualitative and quantitative methods applied to data acquired at high or low temporal resolution[11]. Common to all approaches is the serial acquisition of heavily T_1-weighted images before, during, and after the injection of a contrast agent. In the clinical setting, great emphasis is placed on obtaining DCE-MRI data at high spatial resolution, where it is frequently noted that acquiring data at lower spatial resolution leads to the possibility of missing smaller tumors and mischaracterizing complex lesions[12–15]. Using current methods, high spatial resolution necessitates lower temporal resolution so that the resulting signal-intensity time series can only be analyzed qualitatively or semiquantitatively to characterize general curve-shape features (i.e., washout, plateau, or persistence)[16]. Unfortunately, high temporal resolution DCE-MRI data are required[17,18] for quantitative analysis whereby the dynamic signal-intensity curves are fit to pharmacokinetic models to return estimates of the volume transfer constant (termed K^{trans}; an estimate of tumor vessel blood flow and permeability),

the plasma volume fraction (v_p), and the extravascular extracellular volume fraction (v_e). An example of this can be seen in Fig. 3. Fig. 3a) shows a standard-of-care dynamic breast examination and the associated signal-intensity time course, while Fig. 3b shows a research-based dynamic breast examination used for predicting the response of an invasive ductal carcinoma to therapy. Both images were acquired with heavily T_1-weighted spoiled gradient-echo sequences. In addition to the obvious differences (field of view, and presence or absence or fat saturation), the key point to observe is that the image on the left employed a $448 \times 448 \times 129$ matrix for a spatial resolution of $0.59\,mm^3$ and required approximately 91 s to acquire, whereas the image on the right employed a $192 \times 192 \times 20$ matrix for a spatial resolution of $8.9\,mm^3$ and required 16 s to acquire. Thus, there is a large disparity of spatial and temporal resolution between the dynamic scans acquired for typical standard-of-care assessment and that for a typical research study.

In principle, quantitative analysis of DCE-MRI data from a high temporal resolution MR acquisition should yield the most detail on tumor vascular status. Unfortunately, clinically acquired DCE-MRI data is not optimized for quantitative modeling, thereby greatly impeding the development—and translation—of new and promising DCE-MRI approaches. To see this, observe the down-sampled signal-intensity time course pictured in Fig. 3b (dashed line); the native 16-s temporal resolution has been down-sampled to approximate that of the clinical standard-of-care acquisition. When this is done, much of the structure of the dynamic curve is lost, thereby introducing significant errors in any subsequent pharmacokinetic analysis. If data could be acquired simultaneously with both high spatial and temporal
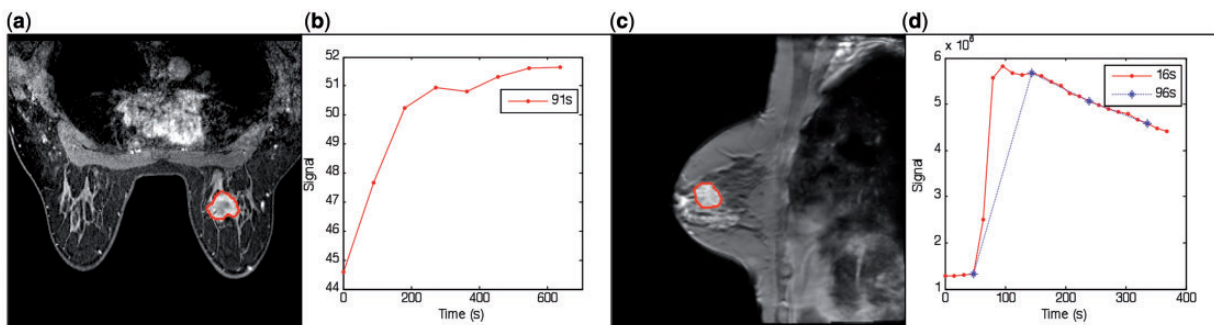
Figure 3   (a) An axial, bilateral, post-contrast, fat-saturated T_1-weighted image with the tumor outlined in red on the left breast. The corresponding signal-intensity time course is presented in (b). These represent fairly standard data available from a clinical examination; while the spatial resolution is quite high (approximately, $0.59\,mm^3$), the temporal resolution is 91 s. (c, d) The analogous data (without fat saturation and with a sagittal field of view) available from a research study; observe the lower spatial resolution (approximately $8.9\,mm^3$). The temporal resolution is 16 s, thereby enabling better characterization of the contrast uptake as needed for pharmacokinetic modeling. Of note is the red line in (d), which shows (approximately) what the signal enhancement curve would look like if the temporal resolution was decreased to that of the clinical scan on the left: the rapid initial rise is substantially underestimated. This simple example elucidates the need for acquisition methods that can simultaneously provide high temporal and high spatial resolution data.

resolution, then DCE-MRI could provide images appropriate for both standard-of-care and research analyses. This would substantially accelerate the development of new, quantitative DCE-MRI methods and enable their rapid transition to clinical use.

While some investigators are realizing the potential power of CS to improve dynamic imaging (see, e.g., Refs,[25−27]), there has been extremely limited application for striking a compromise between the competing acquisition demands of clinical and research examinations. As we[51] and others[52,53] have shown in preliminary (retrospective) investigations, it may be possible to substantially improve the spatial and temporal resolution at which quantitative imaging data are acquired with almost no penalty to the accuracy of the parameters. This has striking implications for the clinical utility of dynamic MRI; in particular, the ability to return estimates of physiologically meaningful pharmacokinetic parameters at high spatial resolution for direct comparison of lesion morphology. There is little doubt that improving spatial resolution in DCE-MRI without sacrificing temporal resolution would enhance our ability to diagnose, assess, and predict the response of tumors to therapy.

The simplest strategy for merging the clinical and research goals would be to accelerate the acquisition of the high spatial resolution clinical scan with CS by omitting a large percentage of k-space from the acquisition and reconstructing with a CS scheme that uses both spatial and temporal constraints. If the dynamic scan time of the clinical scan is roughly a factor of 6 longer than the research scan (91 s vs 16 s), then a factor of 6 acceleration from the CS technique would be sufficient to create a protocol that would work for all patients and allow research data to be collected simultaneously. Similar levels of acceleration have already been demonstrated in both[52,53].

Dynamic susceptibility contrast MRI

DSC-MRI involves the serial and rapid acquisition of T_2- or T_2*-weighted images before, during, and after the bolus injection of a contrast agent to assess hemodynamic information (e.g., blood flow and blood volume) in normal or tumor-bearing brain. Such methods require sufficient temporal resolution to track the first pass of a contrast agent through vessels (<1.5 s per image)[54]. Consequently, the spatial resolution of DSC-MRI is typically lower than that used with DCE- or DWI-MRI, which potentially limits its capability to adequately assess hemodynamic heterogeneity within tumors. The limited spatial resolution of DSC-MRI is particularly relevant given its increasing use to track hemodynamic changes following conventional or antiangiogenic therapy[55,56].

Similarly, the integration of DSC-MRI derived blood flow and blood volume maps into multiparametric analysis methods, such as parametric response mapping[57],

could potentially be hindered by disparities in spatial resolution between the different acquisition methods. The high temporal resolution requirements also limit the spatial coverage achieved by DSC-MRI scans, with many routine clinical implementations (those lacking phased-array technology or specialized sequences) only able to image slices that encompass the tumor-bearing region. Thus, there is a compelling need to develop DSC-MRI acquisition methods capable of high spatial and temporal resolution with large fields of view.

The use of CS acquisition schemes could also benefit advanced DSC-MRI methods that aim to assess physiologic parameters beyond blood flow and blood volume. Such methods typically require more acquisition time, which limits their spatial resolution and coverage. For example, the simultaneous acquisition of gradient and spin-echo DSC-MRI data enables the evaluation of hemodynamic parameters sensitive to the total vasculature and microvasculature, respectively, as well as the measurement of the mean vessel size in a voxel[58,59]. To reduce the effects of contrast agent leakage in brain tumors, DSC-MRI data is increasingly acquired using 2 or more gradient echoes[61,62]. Such an approach also enables the quantification of the T_1 contribution to the DSC-MRI signal and the associated DCE-MRI parameters, K^{trans} and v_e[62]. Similar to the DCE-MRI and DW-MRI methods described earlier, these advanced DSC-MRI methods could greatly benefit from increased spatial resolution and tissue coverage in order to more fully account for tumor spatial heterogeneity and better characterize a tumor's response to treatment.

CS reduces the data acquisition requirements for a given spatial resolution, so if one considers examination time to be fixed, the time saved may be used to acquire additional, higher, spatial frequencies in k-space than were included in the original acquisition, thereby increasing the effective spatial resolution of the data. For Cartesian acquisitions, this could be as simple as increasing the maximum phase-encoded spatial frequency used, leading to a higher effective resolution in the phase encode direction(s). Care must be taken when increasing the spatial resolution in the readout direction, since this will necessitate a decrease in sampling time (increase in sampling bandwidth) for each point and a consequent loss of SNR. Balancing these considerations is part of the planning and optimization process that must precede CS-based acquisition strategies.

Discussion

The potential of CS in qMRI may be limited primarily by how innovatively one uses prior information. For example, in multiecho MRI scans, incorporating the similarity between images of different echo times can allow acceleration of the scan. However, if the reconstruction of the images is performed with inadequate a priori constraints, the algorithm may produce blurred T_2 maps or inaccurate

T_2 estimates. Designing a CS-optimized MRI protocol then becomes an exercise in strategic measurement planning. Even the choice between advanced qMRI measurement approaches, such as Look-Locker or DESPOT1 for T_1 mapping, is a factor to study regarding how well the selected CS reconstruction algorithm can handle partial data sets of each sequence.

One obvious future improvement to the reconstruction side of CS MRI is the development of new priors that are tailored to anatomic imaging with current state-of-the-art MRI protocols. A useful prior (1) has compression artifacts with minimal influence on the diagnostic quality of images and on the error in quantitative parameters; (2) is robust to anatomic variation; (3) is relatively independent of spatial resolution and image contrast; (4) is compatible with parallel imaging, partial Fourier, and partial echo techniques, so as to retain those already significant acceleration factors; and (5) fails gracefully in the presence of increasing levels of noise.

The acquisition side of CS can be improved with better understanding of the optimal way to sample k-space for a given protocol. Tuning sampling patterns to be robust to scan-to-scan variation and to anatomic variation will improve clinical reliability. There is a plethora of sub-sampled k-space acquisition trajectories, from Cartesian to spiral, that have yet to be tested with CS to find the best candidates in terms of data collection efficiency, artifact behavior, and adequate spatial frequency collection.

A better understanding of the limiting factors in standard qMRI protocols will pave the way for CS improvements. Additional investigation of basic CS sparsity constraints, such as total variation and wavelets, is needed to determine which aspects of the more common qMRI protocols are the best candidates for acceleration. Most protocols are already well balanced in terms of spatial resolution, temporal resolution, and SNR. Thus, the reduction of data collection provided by CS will require finding a new balance if one is to aim for minimum error in measured quantitative parameters.

Finally, although almost all CS methods are designed around l_1-norm minimization, mathematically the l_0-norm is preferred in almost all situations because of its relaxed sampling requirement and better performance. Unfortunately, the l_0-norm minimization problem is computationally intractable, so various approximate methods must be employed[63,64]. In the future, CS qMRI could benefit from a shift toward l_0 as the norm of choice if a competitive workaround is found.

Conclusions

CS allows in many cases a reduction of the data collection burden in qMRI protocols, thereby freeing time to collect additional data that directly improve the capabilities of the technique. By incorporating CS into the acquisition of MRI data, it may be possible to capture both high spatial resolution data (for morphology and anatomic assessment) and high temporal resolution, multiparametric data. This would represent a substantial change in the field of cancer imaging, as current quantitative imaging methods are not readily compatible with clinical reality. For example, the competing demands of clinical and research DCE-MRI studies may be able to be addressed by CS methods, as well as the need to acquire DSC-MRI data with increased spatial resolution. To achieve the routine use of CS acceleration for quantitative cancer imaging, a number technical issues related to understanding the properties of CS and the practical implementation must first be addressed, but these are not insurmountable.

In conclusion, we believe that CS offers a reasonable means to overcome fundamental barriers to the practical deployment of quantitative imaging methods in clinical trials and (ultimately) in clinical care.

Acknowledgements

Conflict of interest

The authors declare that they have no conflicts of interest.

References

[1] Candès EJ, Tao T. Near optimal signal recovery from random projections: universal encoding strategies? IEEE Trans Inf Theory 2006; 52: 5406–5425.

[2] Donoho DL. Compressed sensing. IEEE Trans Inf Theory 2006; 52: 1289–1306.

[3] Candès EJ, Romberg J, Tao T. Robust uncertainty principles: exact signal reconstruction from highly incomplete frequency information. IEEE Trans Inf Theory 2006; 52: 489–509.

[4] Lustig M, Donoho DL, Santos JM, Pauly JM. Compressed sensing MRI. IEEE Sig Proc Mag 2008; 25: 72–82.

[5] Lustig M, Donoho D, Pauly JM. Sparse MRI: the application of compressed sensing for rapid MR imaging. Magn Reson Med 2007; 58: 1182–1195.

[6] Gamper U, Boesiger P, Kozerke S. Compressed sensing in dynamic MRI. Magn Reson Med 2008; 59: 365–373.

[7] Jung H, Sung K, Nayak KS, Kim EY, Ye JC. k-t FOCUSS: a general compressed sensing framework for high resolution dynamic MRI. Magn Reson Med 2009; 61: 103–116.

[8] Hu S, Lustig M, Chen AP, et al. Compressed sensing for resolution enhancement of hyperpolarized 13C flyback 3D-MRSI. J Mag Reson 2008; 192: 258–264.

[9] Hu S, Lustig M, Balakrishnan A, et al. 3D compressed sensing for highly accelerated hyperpolarized (13)C MRSI with in vivo applications to transgenic mouse models of cancer. Magn Reson Med 2010; 63: 312–231.

[10] Ajraoui S, Lee KJ, Deppe MH, Parnell SR, Parra-Robles J, Wild JM. Compressed sensing in hyperpolarized 3He lung MRI. Magn Reson Med 2010; 63: 1059–1069.

[11] Doneva M, Börnert P, Eggers H, Stehning C, Sénégas J, Mertins A. Compressed sensing reconstruction for magnetic resonance parameter mapping. Magn Reson Med 2010; 64: 1114–1120.

[12] Doneva M, Börnert P, Eggers H, Mertins A, Pauly J, Lustig M. Compressed sensing for chemical shift-based water-fat separation. Mag Reson Med 2010; 64: 1749–1759.

[13] Otazo R, Kim D, Axel L, Sodickson DK. Combination of compressed sensing and parallel imaging for highly accelerated first-pass cardiac perfusion MRI. Magn Reson Med 2010; 64: 776–776.

[14] Jung H, Ye JC. Motion estimated and compensated compressed sensing dynamic magnetic resonance imaging: what we can learn from video compression techniques. Int J Imaging Systems Technol 2010; 20: 81–98.

[15] Michailovich O, Rathi Y, Dolui S. Spatially regularized compressed sensing of diffusion MRI data. Psychiatry: Interpers Biol Proc 2010; 1: arXiv:1009.1889.

[16] Adluru G, Tasdizen T, Schabel MC, DiBella EVR. Reconstruction of 3D dynamic contrast-enhanced magnetic resonance imaging using nonlocal means. J Magn Reson Imaging 2010; 32: 1217–1227.

[17] Chen L, Schabel MC, DiBella EVR. Reconstruction of dynamic contrast enhanced magnetic resonance imaging of the breast with temporal constraints. Magn Reson Imaging 2010; 28: 637–645.

[18] Wang H, Miao Y, Zhou K, et al. Feasibility of high temporal resolution breast DCE-MRI using compressed sensing theory. Med Phys 2010; 37: 4971.

[19] Bilgic B, Goyal VK, Adalsteinsson E. Multi-contrast reconstruction with Bayesian compressed sensing. Magn Reson Med 2011; 66: 1601–1615.

[20] Moghari MH, Akçakaya M, O'Connor A, et al. Compressed-sensing motion compensation (CosMo): a joint prospective-retrospective respiratory navigator for coronary MRI. Magn Reson Med 2011; 66: 1674–1681.

[21] Wu B, Li W, Guidon A, Liu C. Whole brain susceptibility mapping using compressed sensing. Magn Reson Med 2012; 67: 137–147.

[22] Menzel MI, Tan ET, Khare K, et al. Accelerated diffusion spectrum imaging in the human brain using compressed sensing. Magn Reson Med 2011; 66: 1226–1233.

[23] Trzasko JD, Haider CR, Borisch EA, et al. Sparse-CAPR: Highly accelerated 4D CE-MRA with parallel imaging and nonconvex compressive sensing. Magn Reson Med 2011; 66: 1019–1032.

[24] Trzasko JD, Bao Z, Manduca A, McGee KP, Bernstein MA. Sparsity and low-contrast object detectability. Magn Reson Med 2012; 67: 1022–1032.

[25] Akçakaya M, Nam S, Hu P, et al. Compressed sensing with wavelet domain dependencies for coronary MRI: a retrospective study. IEEE Trans Med Imaging 2011; 30: 1090.

[26] Lee H, Lee DS, Kang H, Kim BN, Chung MK. Sparse brain network recovery under compressed sensing. IEEE Trans Med Imaging 2011; 30: 1154–1165.

[27] Guerquin-Kern M, Haberlin M, Pruessmann KP, Unser M. A fast wavelet-based reconstruction method for magnetic resonance imaging. IEEE Trans Med Imaging 2011; 30: 1649–1660.

[28] Montefusco LB, Lazzaro D, Papi S, Guerrini C. A fast compressed sensing approach to 3D MR image reconstruction. IEEE Trans Med Imaging 2011; 30: 1064–1075.

[29] Chan RW, Ramsay EA, Cheung EY, Plewes DB. The influence of radial undersampling schemes on compressed sensing reconstruction in breast MRI. Magn Reson Med 2012; 67: 363–377.

[30] Ravishankar S, Bresler Y. MR image reconstruction from highly undersampled k-space data by dictionary learning. IEEE Trans Med Imaging 2011; 30: 1028–1041.

[31] Miller AB, Hoogstraten B, Staquet M, Winkler A. Reporting results of cancer treatment. Cancer 1981; 47: 207–214.

[32] Therasse P, Arbuck SG, Eisenhauer EA, et al. New guidelines to evaluate the response to treatment in solid tumors. European Organization for Research and Treatment of Cancer, National Cancer Institute of the United States, National Cancer Institute of Canada. J Natl Cancer Inst 2000; 92: 205–216.

[33] Eisenhauer EA, Therasse P, Bogaerts J, et al. New response evaluation criteria in solid tumours: revised RECIST guideline (version 1.1). Eur J Cancer 2009; 45: 228–247.

[34] Cheson BD, Horning SJ, Coiffier B, et al. Report of an international workshop to standardize response criteria for non-Hodgkin's lymphomas. NCI Sponsored International Working Group. J Clin Oncol 1999; 17: 1244.

[35] Cheson BD, Pfistner B, Juweid ME, et al. Revised response criteria for malignant lymphoma. J Clin Oncol 2007; 25: 579–586.

[36] Erasmus JJ, Gladish GW, Broemeling L, et al. Interobserver and intraobserver variability in measurement of non-small-cell carcinoma lung lesions: implications for assessment of tumor response. J Clin Oncol 2003; 21: 2574–2582.

[37] Ratain MJ, Eckhardt SG. Phase II studies of modern drugs directed against new targets: if you are fazed, too, then resist RECIST. J Clin Oncol 2004; 22: 4442–4425.

[38] Tuma RS. Sometimes size doesn't matter: reevaluating RECIST and tumor response rate endpoints. J Natl Cancer Inst 2006; 98: 1272–1274.

[39] Leach MO, Brindle KM, Evelhoch JL, et al. Assessment of antiangiogenic and antivascular therapeutics using MRI: recommendations for appropriate methodology for clinical trials. Br J Radiol 2003; 76(Suppl): S87–S91.

[40] Padhani AR, Liu G, Koh DM, et al. Diffusion-weighted magnetic resonance imaging as a cancer biomarker: consensus and recommendations. Neoplasia 2009; 11: 102–125.

[41] Kwock L, Smith JK, Castillo M, et al. Clinical role of proton magnetic resonance spectroscopy in oncology: brain, breast, and prostate cancer. Lancet Oncol 2006; 7: 859–868.

[42] Rodrigues LM, Howe FA, Griffiths JR, Robinson SP. Tumor R2* is a prognostic indicator of acute radiotherapeutic response in rodent tumors. J Magn Reson Imaging 2004; 19: 482–488.

[43] Nass SJ, Moses HL, Mendelsohn J, editors. A national cancer clinical trials system for the 21st century: reinvigorating the NCI Cooperative Group Program. National Academies Press; 2010.

[44] Figueiras RG, Padhani AR, Goh VJ, et al. Novel oncologic drugs: what they do and how they affect images. Radiographics 2011; 31: 2059–2091.

[45] Smith DS, Li X, Gambrell JV, et al. Robustness of quantitative compressive sensing MRI: the effect of random undersampling patterns on derived parameters for DCE- and DSC-MRI. IEEE Trans Med Imag 2012; 31: 504–511.

[46] Trzasko JD, Haider CR, Borisch EA, et al. Sparse-CAPR: highly accelerated 4D CE-MRA with parallel imaging and nonconvex compressive sensing. Mag Reson Med 2011; 66: 1019–1032.

[47] Trzasko JD, Bao Z, Manduca A, McGee KP, Bernstein MA. Sparsity and low-contrast object detectability. Mag Reson Med 2012; 67: 1022–1032.

[48] Buehrer M, Pruessmann KP, Boesiger P, Kozerke S. Array compression for MRI with large coil arrays. Magn Reson Med 2007; 57: 1131–1139.

[49] Smith DS, Gore JC, Yankeelov TE, Welch EB. Real-time compressive sensing MRI reconstruction using GPU computing and split Bregman methods. Int J Biomed Imag 2012; Article ID 864827: Epub 2012 Feb 1.

[50] Murphy M, Alley M, Demmel J, Keutzer K, Vasanawala S, Lustig M. Fast l_1-SPIRiT compressed sensing parallel imaging

MRI: scalable parallel implementation and clinically feasible runtime. IEEE Trans Med Imaging 2012; 31: 1250–1262.

[51] Smith DS, Welch EB, Li X, et al. Quantitative effects of using compressed sensing in dynamic contrast enhanced MRI. Phys Med Bio 2011; 56: 4933–4946.

[52] Wang H, Miao Y, Zhou K, et al. Feasibility of high temporal resolution breast DCE-MRI using compressed sensing theory. Med Phys 2010; 37: 4971.

[53] Chan RW, Ramsay EA, Cheung EY, Plewes DB. The influence of radial undersampling schemes on compressed sensing reconstruction in breast MRI. Mag Reson Med 2012; 67: 363–377.

[54] Østergaard L. Principles of cerebral perfusion imaging by bolus tracking. J Magn Reson Imaging 2005; 22: 710–717.

[55] Batchelor TT, Sorensen AG, di Tomaso E, et al. AZD2171, a pan-VEGF receptor tyrosine kinase inhibitor, normalizes tumor vasculature and alleviates edema in glioblastoma patients. Cancer Cell 2007; 11: 83–95.

[56] Quarles CC, Schmainda KM. Assessment of the morphological and functional effects of the anti-angiogenic agent SU11657 on 9L gliosarcoma vasculature using dynamic susceptibility contrast MRI. Magn Reson Med 2007; 57: 680–687.

[57] Tsien C, Galbán CJ, Chenevert TL, et al. Parametric response map as an imaging biomarker to distinguish progression from pseudoprogression in high-grade glioma. J Clin Oncol 2010; 28: 2293–2299.

[58] Weisskoff RM, Zuo CS, Boxerman JL, Rosen BR. Microscopic susceptibility variation and transverse relaxation: theory and experiment. Magnetic Reson Med 1994; 31: 601–610.

[59] Troprès I, Grimault S, Vaeth A, et al. Vessel size imaging. Magnetic Reson Med 2001; 45: 397–408.

[60] Vonken EJ, van Osch MJ, Bakker CJ, Viergever MA. Measurement of cerebral perfusion with dual-echo multi-slice quantitative dynamic susceptibility contrast MRI. J Magn Reson Imaging 1999; 10: 109–117.

[61] Sourbron S, Heilmann M, Biffar A, et al. Bolus-tracking MRI with a simultaneous T1- and T2*-measurement. Magnetic Reson Med 2009; 62: 672–681.

[62] d'Arcy JA, Collins DJ, Rowland IJ, Padhani AR, Leach MO. Applications of sliding window reconstruction with cartesian sampling for dynamic contrast enhanced MRI. NMR Biomed 2002; 15: 174–183.

[63] Chartrand R. Fast algorithms for nonconvex compressive sensing: MRI reconstruction from very few data. 2009 IEEE International Symposium on Biomedical Imaging: From Nano to Macro. Boston, MA: IEEE Press; 2009, p. 262–265.

[64] Trzasko J, Haider C, Manduca A. Practical Nonconvex compressive sensing reconstruction of highly-accelerated 3d parallel mr angiograms. 2009 IEEE International Symposium on Biomedical Imaging: From Nano to Macro. Boston, MA: IEEE Press; 2009, p. 274–277.